Electronic Supplementary Material (ESI) for Nanoscale Advances.

Electronic Supplementary Information

Observing quantum trapping on MoS_2 through the lifetimes of resonant electrons: revealing the Pauli exclusion principle

Wei-Bin Su,*[a] Shin-Ming Lu,[a] Horng-Tay Jeng,*[b,a,c] Wen-Yuan Chan,[a] Ho-Hsiang Chang,[a] Woei Wu Pai,[d] Hsiang-Lin Liu[e] and Chia-Seng Chang[a]

[a] *Institute of Physics, Academia Sinica, Nankang, Taipei 11529, Taiwan*

[b] *Department of Physics, National Tsing Hua University, Hsinchu 30013, Taiwan*

[c] *Physics Division, National Center for Theoretical Sciences, Hsinchu 30013, Taiwan*

[d] *Center for Condensed Matter Sciences, National Taiwan University, Taipei 10617, Taiwan*

[e] *Department of Physics, National Taiwan Normal University, Taipei 11677, Taiwan*

E-mail: wbsu@phys.sinica.edu.tw; jeng@phys.nthu.edu.tw

Supplementary Note 1. Spectra due to spontaneous changes of tip sharpness

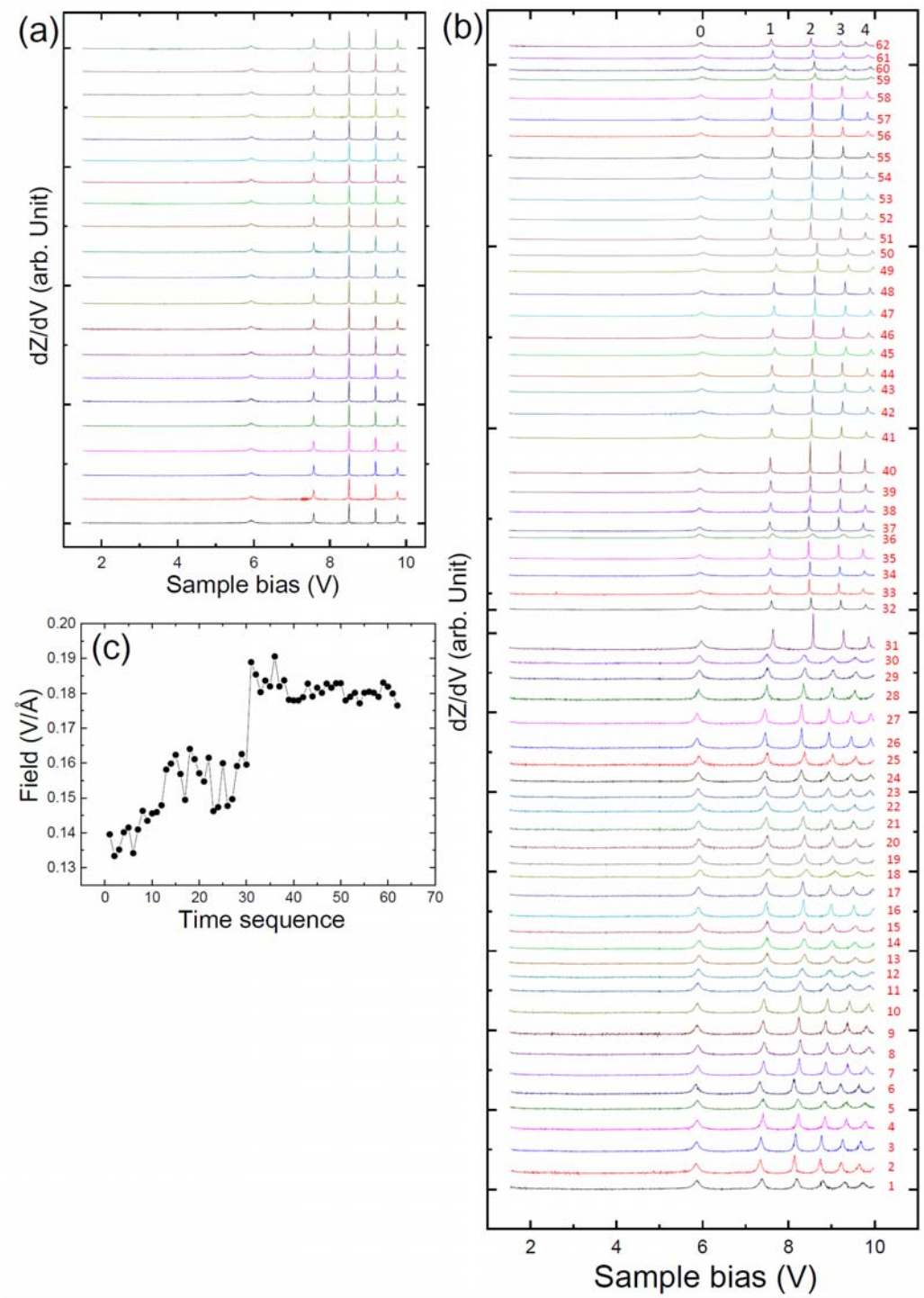

Figure S1. (a) Similar spectra before the sharpness changed. (b) Spectra with FERs of different shapes and energies due to spontaneous changes of tip sharpness. The numbers at the right-hand side indicate a time sequence of different spectra. (b) F_{FER} for FERs in each spectrum in (b) versus time sequence, revealing that F_{FER} was fluctuated with time. F_{FER} for FERs in each spectrum was calculated by Eq. (1) in the text.

Supplementary Note 2. Observing FER linewidth on Ag(100) surface

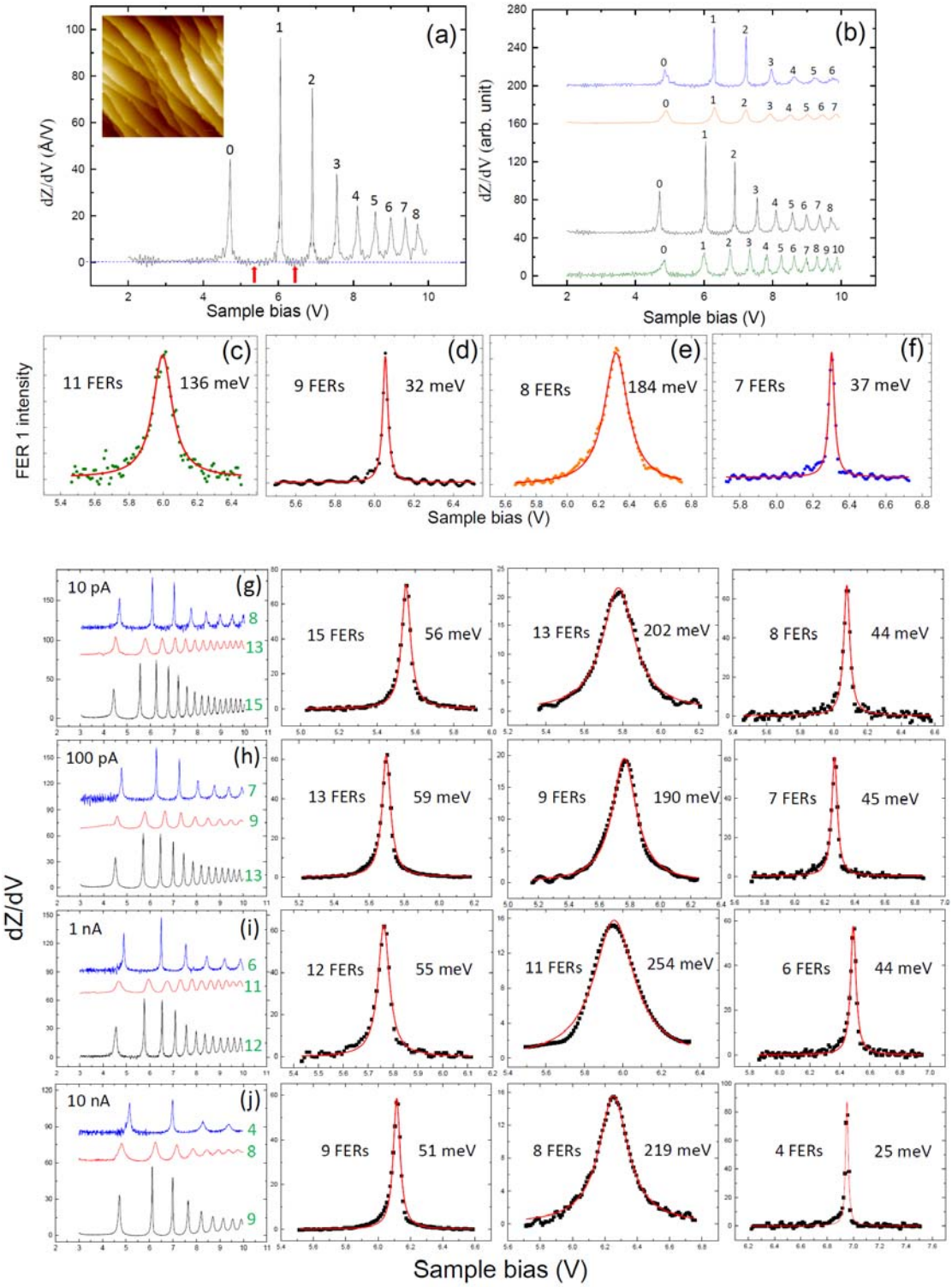

Figure S2. (a) A differential *Z*-*V* spectrum with nine FER peaks marked by numbers. Zero spectral intensity is indicated by a dashed line, revealing that the intensities of valleys (marked by arrows) around the peak of FER 1 are zero. Inset: a typical STM image of the Ag(100) surface. The image size is 100 nm×100 nm. (b) Differential *Z*-*V* spectra with seven, eight, nine, and 11 FERs. (c)-(f) Lorentzian

fittings of FER 1 in (b). The linewidths extracted from the fittings modulate with the FER numbers. FER spectra were acquired at 78 K under 10 pA. (g)–(j) FER spectra with different FER number acquired at 5 K under 10 pA, 100 pA, 1 nA, and 10 nA, respectively, and Lorentzian fittings of FER 1, showing the linewidth modulation with the number of FERs.

Supplementary Note 3. Observing FER linewidth on Ag(111) surface

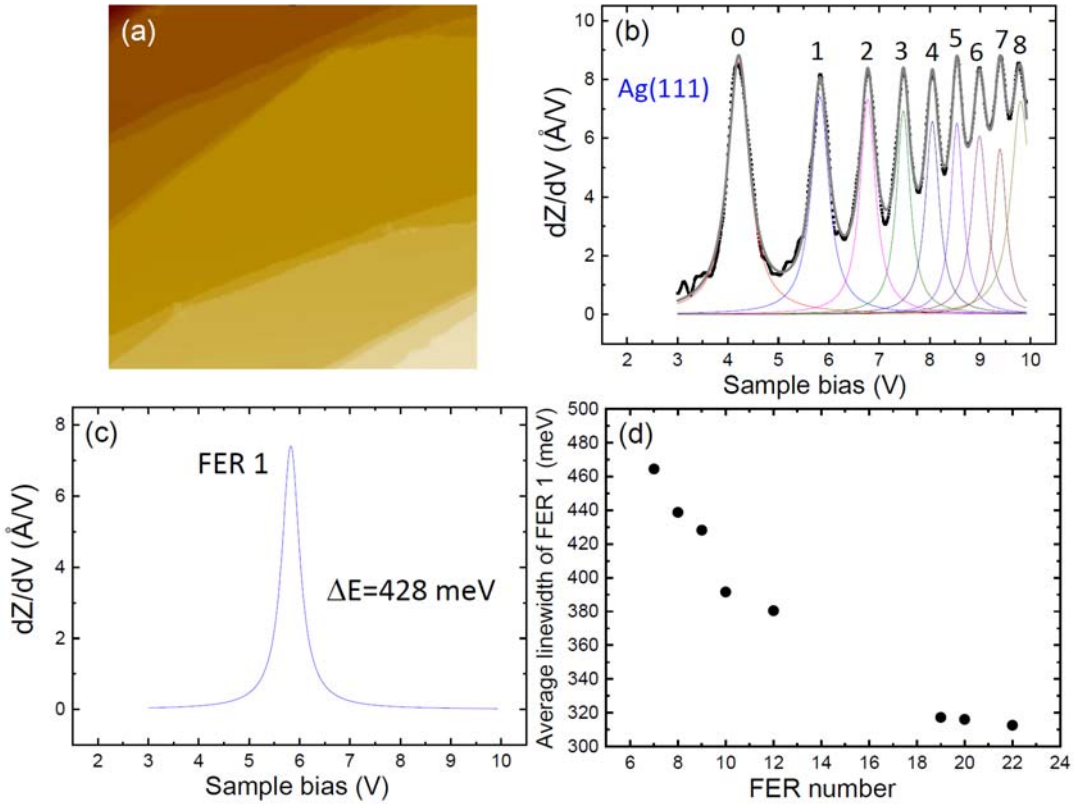

Figure S3. (a) A typical STM image of the Ag(111) surface. The image size is 100 nm×100 nm. (b) A differential *Z*-*V* spectrum with nine FER peaks marked by numbers. Zero valley intensity is not observed because of no band gap. (c) Lorentzian fittings of FER 1 in (b). Average linewidth of FER 1 versus FER number, showing that the average linewidth decreases with the number monotonically. Because of no band gap, the FER electron can transmit through the surface due to the density of states (Ref. 21). As a result, the probability that a relaxed electron coexists with an FER electron would decrease, and the probability that the relaxed electron engaging in resonance trapping largely prolongs the lifetime of resonant electrons would be also substantially reduced. The linewidth modulation vanishes on Ag(111) surfaces accordingly.

Supplementary Note 4. Correlation between the tip sharpness and electric field of FERs

The tip sharpness leads to F_{FE} for field emission being stronger than F_{FER} for FERs. If we define a factor $f = F_{FE} / F_{FER}$, then f is larger than 1 for an STM tip, and f is larger when the tip is sharper. For a planar tip, $f = 1$ because F_{FE} is equal to F_{FER} in this case. In our experiment, the set current was the same for acquiring spectra with various numbers of FERs. Therefore, the electric field F_{FE} of generating field emission current was the same for any sharpness. As a result, $F_{FE} = f F_{FER}$ is a constant, and f is inversely proportional to F_{FER}. Accordingly, a sharper tip corresponds to a weaker F_{FER}.

Moreover, under the same applied voltage and distance between the tip and sample, F_{FE} is stronger, and more field emission current can be generated for a sharper tip. Therefore, for the same current, the distance should be larger for a sharper tip. Figure S3 depicts Z-V spectra with three, four, and five FERs shown as step features. Because the Z-V spectrum provides information on the distance between the tip and sample, Fig. S3 reveals that the distance enlarged with increasing the number of FERs when the tip was in the state of field emission (bias voltage > 6 V). Therefore, this result indicates that a sharper tip corresponds to a weaker F_{FER}.

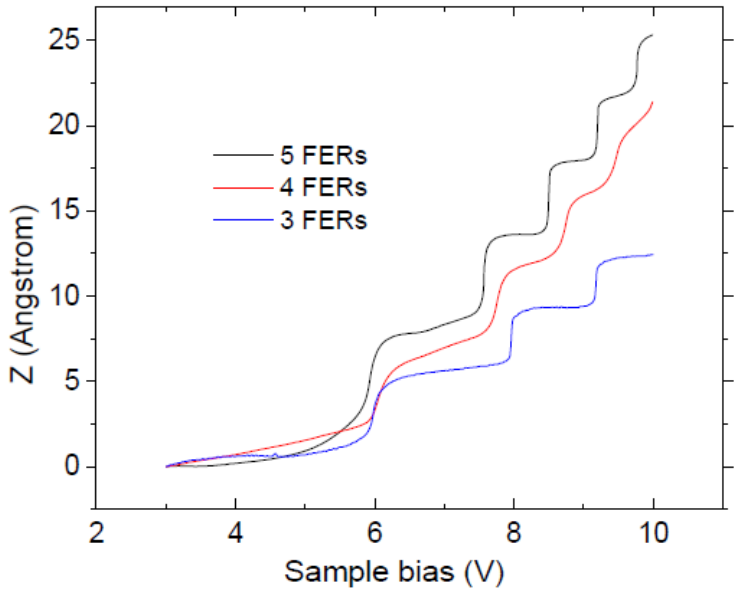

Figure S4. Z-V spectra with three, four, and five FERs shown as step features.

Supplementary Note 5. Simulation of the FER spectrum

For simulating the FER spectrum without including the band structure, the potential in the sample is a constant and lower than the vacuum level by V_0, as depicted in Fig. S4, and the potential in STM junction is linear. When electrons at the Fermi level of the tip tunnel into the vacuum, their electronic wave will be partially reflected from the surface (marked 0) due to an abrupt potential change and totally reflected from the classical turning point (marked a). Although field emission electrons will eventually transmit through the surface into the sample interior, they may experience multiple reflection between the surface and the classical turning point before transmitting. As a result, the initial wave function is decomposed into Ψ_t, $\Psi_<$, and $\Psi_>$. Ψ_t is the transmission wave function in the sample, and $\Psi_<$ ($\Psi_>$) is the wave function for electrons moving toward (away) from the surface. When the superposition of $\Psi_<$ and $\Psi_>$ becomes standing waves, quantized states causing FERs are formed, which is similar to the case of the quantum well state (QWS) in the metallic films.

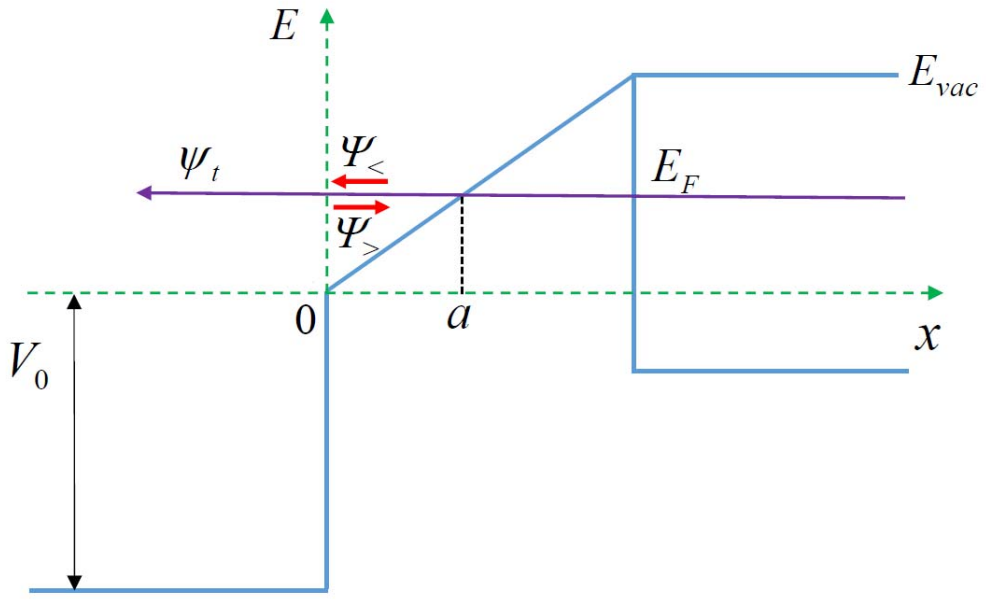

Figure S5. Energy diagram for simulating FER spectra without including the band structure of the sample.

Paggel *et al.* had demonstrated that the QWS spectra can be fit by the absolute square of an interference factor, which is the Fabry Pérot formula for electrons in QWS[1]. Based on this study, we expect that the FER spectra can be simulated by formulating an interference factor for this case, which is

$$\frac{1}{1-r_c r_v e^{i\int_0^a \frac{2\sqrt{2m(E-eFx)}}{\hbar}dx}} \qquad (1)$$

where r_c and r_v are the reflection coefficients at the surface and the classical turning point, respectively. E is the energy of field emission electrons, F is the electric field for field emission, and x is the distance from the surface. In Eq. (1), there is no damping term as in the case of QWS because field emission electrons are in the vacuum. Due to a total reflection from the classical turning point,

$$r_v = e^{-i\frac{\pi}{2}}. \qquad (2)$$

according to previous studies[2,3]. We can obtain r_c from Ψ_t, $\Psi_<$, and $\Psi_>$. The wave function in a linear potential is Airy function,[2] i.e

$$\psi(\mathrm{x}) = CA_j(\xi(x)) + DB_j(\xi(x)) \qquad 0 \le x \le a \qquad (3)$$

where

$$A_j(\xi(x) = \frac{1}{2}(iA_i(\xi(x)) + B_i(\xi(x)))$$

$$B_j(\xi(x) = \frac{1}{2}(A_i(\xi(x)) + iB_i(\xi(x)))$$

$$\xi(x) = (\frac{2meF}{\hbar^2})^{\frac{1}{3}}(x - \frac{E}{eF})$$

$A_j(\xi(x))$ is $\Psi_<$ and $B_j(\xi(x))$ is $\Psi_>$. Ψ_t is simply the plane wave, i.e.

$$\psi(\mathrm{x}) = Ae^{-ikx} \qquad x \le 0 \qquad (4)$$

where $k = \frac{\sqrt{2m(E+V_0)}}{\hbar}$. Since $\Psi(x)$ and d$\Psi(x)$/dx are continuous at $x = 0$,

$$A = CA_j(\xi(0)) + DB_j(\xi(0)) \qquad (5)$$

$$-ikA = C\frac{dA_j(\xi(0))}{dx} + D\frac{dB_j(\xi(0))}{dx} \qquad (6)$$

From Equations (5) and (6), r_c is determined to be[4]

$$r_c = \frac{DB_j(\xi(0))}{CA_j(\xi(0))} = \frac{(-ikA_j(\xi(0)) - \frac{dA_j(\xi(0))}{dx})B_j(\xi(0))}{(ikB_j(\xi(0)) + \frac{dB_j(\xi(0))}{dx})A_j(\xi(0))} \qquad (7)$$

Then the FER spectrum can be simulated by

$$\left| \frac{1}{1 - r_c r_v e^{i\int_0^a \frac{2\sqrt{2m(E-Fx)}}{\hbar} dx}} \right|^2 \qquad (8)$$

Figure S5 is the simulation for the electric field from 0.1 to 0.2 V/Å, displaying the oscillatory characteristic in FER spectra and that the number of FER peaks decreases with increasing the electric field, consistent with experimental observation. Moreover, Fig. S6 displays plots of the energies of FER peaks in Fig. S5 versus $(n\text{-}1/4)^{2/3}$. The results show that the data points can be fit well by the lines corresponding to the set electric fields. Therefore, the simulation is valid. Figure S7 depicts the Lorentzian fittings of the FER peaks of the first order (marked 1) in simulated spectra in Fig. S5, showing that the value of the linewidth extracted from the fitting is larger for a stronger electric field. Therefore, the inverse of the linewidth decreases with increasing the electric filed, as shown in Fig. 3(d). This variation is the same for FER peaks of higher orders.

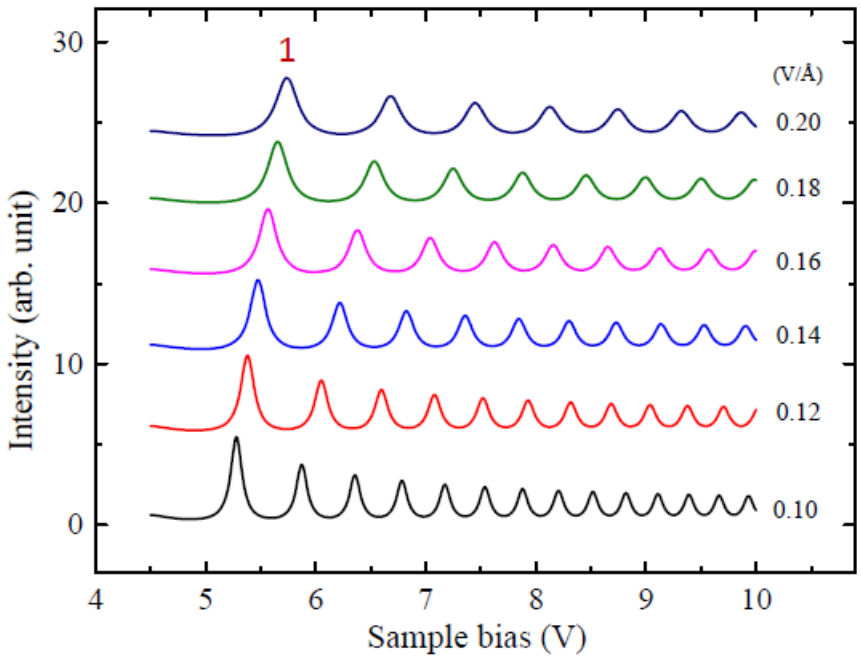

Figure S6. The simulation of FER spectra for the electric field ranging from 0.1 to 0.2 V/Å under $V_0 = 10$ eV and sample work function of 4.5 eV.

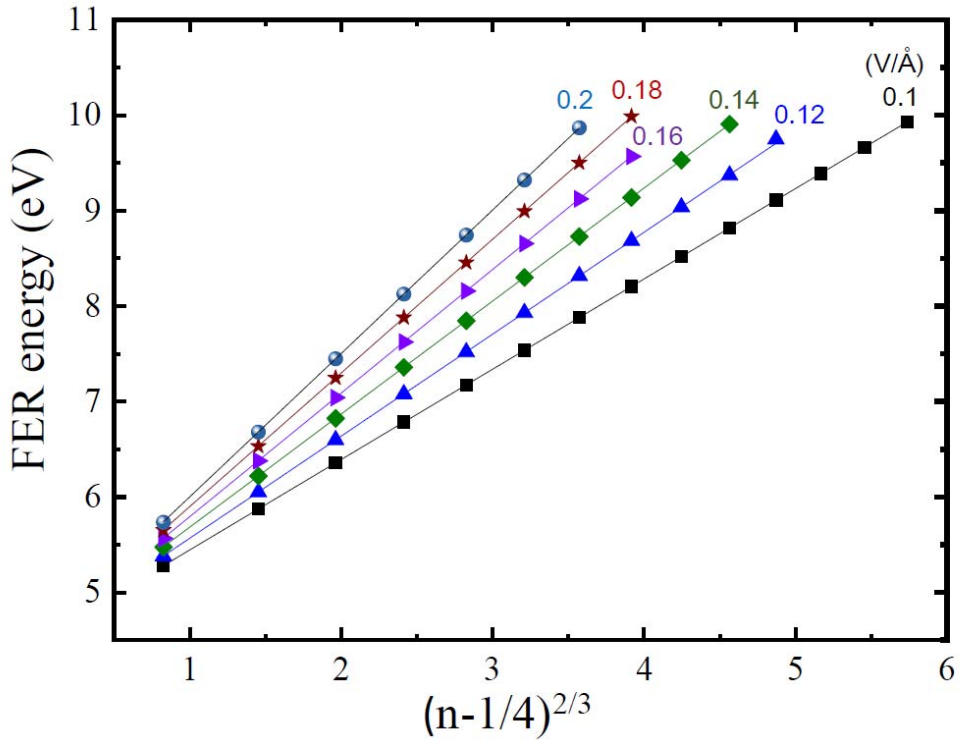

Figure S7. Plots of the energies of FER peaks in Supplementary Figure 3 versus $(n-1/4)^{2/3}$.

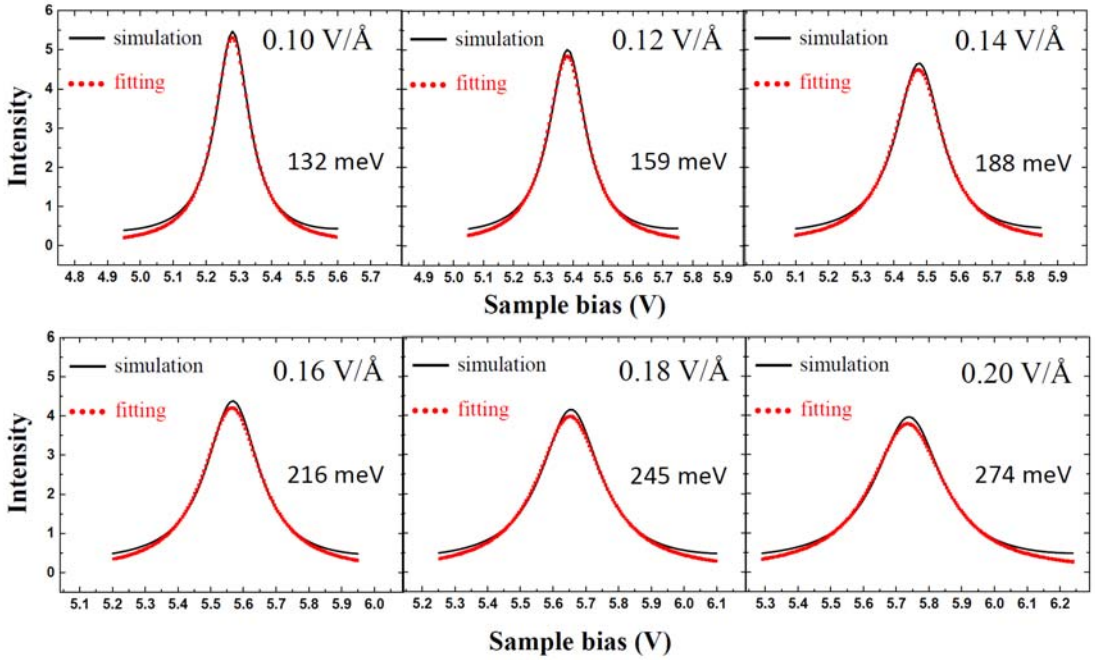

Figure S8. Lorentzian fittings of the FER peaks of the first order (marked 1) in simulated spectra in Supplementary Figure 2.

References of Supplementary Note 5

1. Paggel, J. J., Miller, T. & Chiang, T.-C. Quantum-Well States as Fabry-Pérot Modes in a Thin-Film Electron Interferometer. *Science* **283**, 1709 (1999).
2. Chapman, C. Fundamentals of Seismic Wave Propagation. 1st edn (Cambridge University Press) p 289-291 (2004).
3. Merzbacher, E., Quantum Mechanics. 2nd edn (John Wiley & Sons, Inc. New York) p 123 (1970).

We explain why r_c is equal to $\frac{DB_j(\xi(0))}{CA_j(\xi(0))}$. We use the step potential to illustrate this situation. Firstly, let us assign the step potential to appear at $x = a$. If the wave functions of the incident, reflected, and transmitting waves are $A\mathrm{e}^{-ik_1x}$, $B\mathrm{e}^{ik_1x}$, and $C\mathrm{e}^{-ik_2x}$, respectively, we can obtain $\frac{B}{A} = \frac{(k_1 - k_2)e^{-ik_1a}}{(k_1 + k_2)e^{ik_1a}}$, which is usually viewed as the reflection coefficient. However, $\frac{B}{A}$ is position-dependent because of $\frac{e^{-ik_1a}}{e^{ik_1a}}$, contradictory to that the reflection coefficient should be independent of the position that the step potential occurs. Therefore, we suggest that the real reflection coefficient r_c is $\alpha\frac{B}{A}$, where $\alpha = \frac{e^{ik_1a}}{e^{-ik_1a}}$. As a result, $r_c = \frac{k_1 - k_2}{k_1 + k_2}$ is independent of the position. The fator α is the reflected wave function divided by the incident wave function at $x = a$. Therefore, for the case in Supplementary Figure 1, α becomes $\frac{B_j(\xi(0))}{A_j(\xi(0))}$ for $a = 0$, and therefore $r_c = \frac{DB_j(\xi(0))}{CA_j(\xi(0))}$.

Supplementary Note 6. Emission of two electrons through the exchange interaction

Based on the model of an STM tip in Fig. 2(a), field emission current is emitted from the apex of the protrusion because that is where the electric field is the strongest. Let us model the protrusion as a cone, as shown in Fig. S8(a). The axis (dashed line) of the cone is in the z direction normal to the sample surface. According to the tunneling theory of field emission, which is based on the free electron gas model, electrons at Fermi level E_F of the tip have the highest probability of tunneling through the energy barrier at the metal surface into the vacuum to be the field emission current. Therefore, it is plausible that the resonant electrons in an FER are from the energy state at the Fermi level of the tip. Because the strongest electric field at the apex is in the z direction, the width of the energy barrier in the z direction is the shortest. As a result, electrons in the tip prefer to tunnel along the z direction, and the tunneling probability is only dependent on the electron energy E_z in the z direction.

The tunneling probability is higher for larger E_z because electrons with larger E_z face an energy barrier with a shorter width w and lower height h, as illustrated in Fig. S8 (b). Thus, electrons at the Fermi level have the highest tunneling probability when their energies in the x and y directions (E_x and E_y) are zero. Therefore, resonant electrons in FERs are from the energy state: $E_x = 0$, $E_y = 0$, $E_z = E_F$. This energy state can accommodate two electrons with opposite spins. Let us define electron 1 with spin up and electron 2 with spin down; we suggest that these two electrons can be successively emitted into the quantized state in the FER through exchange interaction.

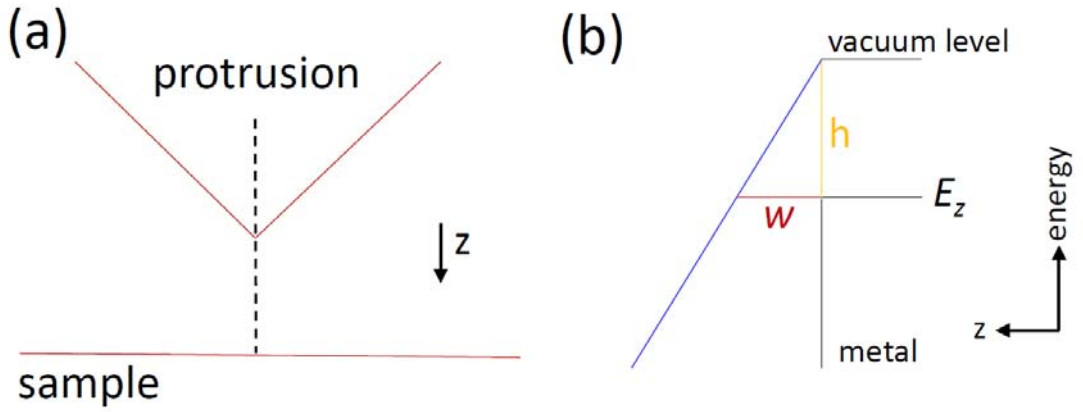

Figure S9. (a) Cone model for protrusion, where a dashed line indicates the axis of the cone in the z direction normal to the sample surface. (b) Energy diagram for field emission.

If electron 1 is emitted first, because of the reflection at the sample, its wave function is a standing wave and a decay wave, as depicted in the upper schematic in Fig. S10. Although electron 2 is not emitted yet, its wave function in the vacuum would not vanish, but would include a decay wave and travelling wave, as displayed in the lower schematic. Evidently, the wave functions of the electrons 1 and 2 overlap in the vacuum. According to quantum mechanics, the exchange interaction exists between electrons 1 and 2 because of the overlap of wave functions, and the total wave function of these two electrons should be antisymmetric. The total wave function is the product of a total space wave function and total spin eigenfunction. Because the spins of electrons 1 and 2 are opposite, the total spin eigenfunction is antisymmetric. As a result, the total space wave function should be symmetric, because of which the probability density of two electrons appearing at the same location is much higher than them being separated.

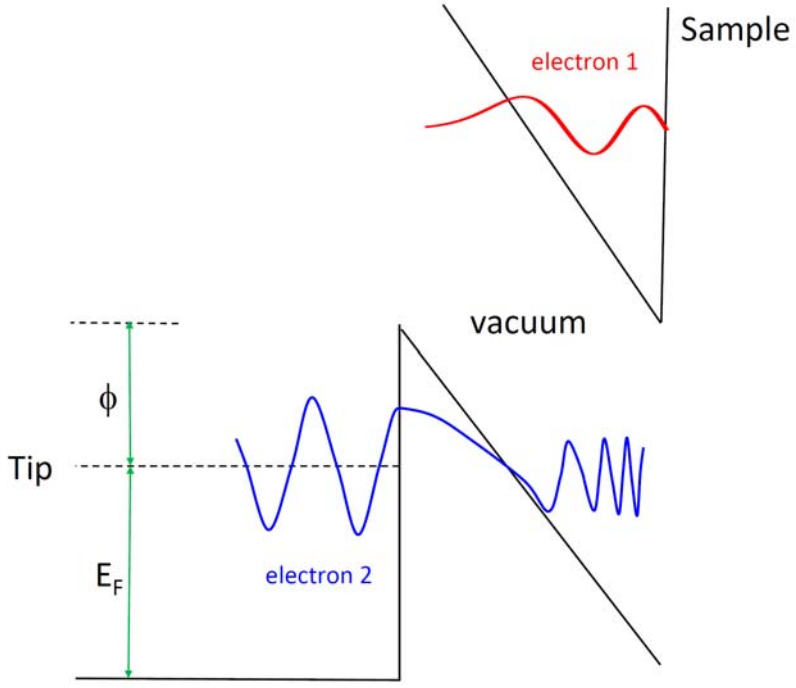

Figure S10. Overlap of the wave functions of a resonant electron in the STM junction and an electron at the Fermi level of the STM tip.

This situation implies that electron 1 can effectively attract electron 2 into vacuum through the exchange interaction, causing the emission of electron 2. To establish a standing wave, electron 1 should motion back and forth for a round trip in the STM junction. Thus, the time interval between the emissions of these two electrons is the round-trip time of electron 1, which, according to the inset in Fig. 3(d), is several

femtoseconds. Because of the exchange interaction, the tunneling process in the FER is two-electron tunneling, which is fundamentally different from one-electron tunneling in normal field emission. However, when the bias voltage of STM is low, the tunneling current is dominated by one-electron tunneling because the wave function in STM junction is simply the evanescent wave.